Molecular Phylogenetics and Evolution 134 (2019) 122–128

Contents lists available at ScienceDirect

Molecular Phylogenetics and Evolution

journal homepage: www.elsevier.com/locate/ympev

Mitogenomic evidence of close relationships between New Zealand's extinct giant raptors and small-sized Australian sister-taxa

Michael Knapp[a,*], Jessica E. Thomas[b,c,1], James Haile[c,1], Stefan Prost[d,e], Simon Y.W. Ho[f], Nicolas Dussex[a,g], Sophia Cameron-Christie[a], Olga Kardailsky[a], Ross Barnett[c], Michael Bunce[h], M. Thomas P. Gilbert[c,i], R. Paul Scofield[j]

[a] Department of Anatomy, University of Otago, 270 Great King Street, Dunedin 9016, New Zealand
[b] Molecular Ecology and Fisheries Genetics Laboratory, School of Biological Sciences, Bangor University, Bangor, UK
[c] Natural History Museum of Denmark, University of Copenhagen, Copenhagen, Denmark
[d] Research Institute of Wildlife Ecology, Vetmeduni Vienna, Vienna, Austria
[e] Department of Integrative Biology, University of California Berkeley, Berkeley, USA
[f] School of Life and Environmental Sciences, University of Sydney, Sydney, Australia
[g] Department of Bioinformatics and Genetics, Swedish Museum of Natural History, Stockholm, Sweden
[h] Trace and Environmental DNA Laboratory, School of Molecular and Life Sciences, Curtin University, Bentley, WA 6102, Australia
[i] Norwegian University of Science and Technology, University Museum, 7491 Trondheim, Norway
[j] Canterbury Museum, 8013 Christchurch, New Zealand

ARTICLE INFO

Keywords:
Ancient DNA
Climate change
Extinction
Island gigantism
New Zealand megafauna
Trans-Tasman dispersal

ABSTRACT

Prior to human arrival in the 13th century, two large birds of prey were the top predators in New Zealand. In the absence of non-volant mammals, the extinct Haast's eagle (*Hieraaetus moorei*), the largest eagle in the world, and the extinct Eyles' harrier (Circus *teauteensis*) the largest harrier in the world, had filled ecological niches that are on other landmasses occupied by animals such as large cats or canines. The evolutionary and biogeographic history of these island giants has long been a mystery. Here we reconstruct the origin and evolution of New Zealand's giant raptors using complete mitochondrial genome data. We show that both Eyles' harrier and Haast's eagle diverged from much smaller, open land adapted Australasian relatives in the late Pliocene to early Pleistocene. These events coincided with the development of open habitat in the previously densely forested islands of New Zealand. Our study provides evidence of rapid evolution of island gigantism in New Zealand's extinct birds of prey. Early Pleistocene climate and environmental changes were likely to have triggered the establishment of Australian raptors into New Zealand. Our results shed light on the evolution of two of the most impressive cases of island gigantism in the world.

1. Introduction

New Zealand's geographic isolation and lack of non-volant mammals has led to a unique avifauna but one that suffered an extinction rate of ~50% following human arrival (Worthy and Holdaway, 2002). Among the most remarkable examples are New Zealand's avian apex predators, Haast's eagle (*Hieraaetus moorei*; formerly *Harpagornis moorei*) and Eyles' harrier (Circus *teauteensis* previously referred to as *C. eylesi*). Both species have long been recognized as examples of island gigantism and filled ecological niches that are on other landmasses occupied by animals such as large cats or canines. Haast's eagle was the largest known eagle in the world and is estimated to have weighed up to 15 kg, significantly more heavy than the largest extant eagle, the harpy (*Harpia harpyja*) at about 9 kg (Worthy and Holdaway, 2002). Haast's eagle remains have so far only been found in the South Island of New Zealand. As an adaptation to the mostly forested New Zealand environment prior to human arrival, its wings were likely broad but with a limited wingspan of about 2.5–3 m (Worthy and Holdaway, 2002). Haast's eagle likely preyed on various large moa species, and adaptation to this previously unoccupied niche is thought to have driven the evolution of the giant body size.

Eyles' harrier was a much lighter bird than Haast's eagle, but with a weight of ~3–3.5 kg it was still the largest known harrier in the world. Its wingspan probably reached 2 m. Unlike Haast's eagle, Eyles' harrier

* Corresponding author.
E-mail address: michael.knapp@otago.ac.nz (M. Knapp).
[1] These authors contributed equally to this work.

https://doi.org/10.1016/j.ympev.2019.01.026
Received 3 October 2018; Received in revised form 22 January 2019; Accepted 31 January 2019
Available online 10 February 2019
1055-7903/

was also found in the North Island of New Zealand, but evidence of its presence is so far lacking from the far south of the South Island. It likely preyed on New Zealand pigeon, kaka, kea and smaller moa species (Worthy and Holdaway, 2002).

The two New Zealand island giants were driven to extinction within the last 700 years, and most workers consider this to be a result of anthropogenic habitat alteration or competition for resources with the growing human population (Bunce et al., 2005; Worthy and Holdaway, 2002).

The evolutionary relationships of Haast's Eagle were resolved by analyses of the mitochondrial cytochrome *b* gene (Bunce et al., 2005). Surprisingly, Haast's eagles were found to belonged to a group of small eagles, including the Australasian little eagle (*Hieraaetus morphnoides*), the smallest eagle in the world, and the also small-bodied Eurasian booted eagle (*Hieraaetus pennatus*). Little eagle weighs less than 1 kg and has a wingspan of 1.1–1.3 m. Booted eagle is only marginally larger. Divergence time estimates suggested that the three lineages diverged less than 2 million years ago (Ma), but estimates were based on a general avian substitution rate, which is known to be highly variable between lineages (Nabholz et al., 2016).

No genetic analyses of the New Zealand Eyles' harrier phylogeny exists. Based on morphological evidence and biogeographic data, Worthy & Holdaway (2002) hypothesised that the taxon was a gigantic relative of the extant swamp harrier (*Circus approximans*), an Australasian native bird. The swamp harrier has arrived in New Zealand naturally at some point in the previous 700 years, potentially filling the niche of the then extinct Eyles' Harrier.

Here we analyse the mitochondrial genomes of Haast's eagle, Eyles's harrier, and their closest relatives to infer a fossil-calibrated phylogenetic tree. This allows us to reconstruct the evolutionary histories of the two New Zealand island giants, along with the environmental and biogeographical changes that are likely to have shaped their evolution.

2. Materials and methods

2.1. Samples and DNA extraction

A subfossil femur from Eyles's Harrier was excavated from Finsch's Folly Tomo a cave near the town of Kimball, in South Canterbury, New Zealand. The remains were not directly dated but were associated with bones of Finsch's duck, Kakapo and Adzebill dated at 1560–1181 years before present (BP) (See (Wood et al., 2017)). We obtained a subfossil right shoulder bone (coracoid) of Haast's eagle, excavated from King's Cave, South (Canterbury Museum number SB24). The remains were not directly dated but were associated with remains of 2150 – 1132 BP (see (Worthy, 1997)). Both samples are held at Canterbury Museum (Christchurch, New Zealand). DNA was extracted and manipulated in dedicated ancient DNA clean-room facilities at the University of Otago and the University of Copenhagen (Knapp et al., 2012). We used the silica based method described by Dabney et al. (2013) for extracting DNA from the Eyles's harrier femur. For extracting DNA from the Haast's eagle coracoid, we used the method described by Leonard et al. (2000) with modifications. SDS and DTT were added in the extraction buffer and instead of using phenol/chloroform, 30 K Amicon Millipore Ultra Centrifugal Filters and Qiagen Minelute columns were used to concentrate and clean the DNA extract. Extraction started from 44 mg of bone material for the Eyles's harrier and 50 mg of bone material for Haast's eagle. No-template controls were conducted alongside each extraction.

Our reconstruction of timescales for the evolution of island giantism required us to estimate divergence times of the New Zealand island giants from their closest relatives. For Haast's eagle these include little eagle and booted eagle, as identified by (Bunce et al., 2005). For Eyles' harrier we identified the spotted harrier (*Circus assimilis*) as closest relative (see Section 2.2). For these extant species, we extracted DNA either from blood samples (booted eagle and little eagle) or tissue samples (spotted harrier). Blood samples were collected from captive individuals during routine veterinary examinations and subsamples of these blood samples were used for DNA analyses. The booted eagle sample came from a bird at the International Centre for Birds of Prey in Newent, United Kingdom. The little eagle sample came from blood donated from Perth Raptor Care. The spotted harrier DNA was extracted from a liver tissue sample provided by the Australian National Wildlife Collection (CSIRO, Canberra, Australia) to Canterbury Museum (registration number B53083). DNA was extracted from blood and tissue samples using the Qiagen blood and tissue kit, following the manufacturer's instructions. DNA was extracted from 10 µL of blood from the samples of little eagle and the booted eagle and from 25 mg of liver tissue from the spotted harrier.

2.2. DNA sequencing

Prior to sequencing complete mitogenomes, we carried out a preliminary analysis to identify the Eyles' harrier's position and its closest relative in the global harrier phylogeny (Oatley et al., 2015). For this purpose, we amplified a 1027 bp mitochondrial region containing the genes encoding tRNA-Leu, NADH dehydrogenase subunit 1 (*ND1*), tRNA-Ile, and tRNA-Gln in six overlapping amplicons (see supplementary table S1). Each fragment was amplified twice and sequenced in both directions on an ABI3730 platform. The consensus was called from all unambiguous sites (i.e. sites for which sequence data from both amplicons were identical).

The five complete mitogenomes presented in this study were sequenced as part of multiple projects with different objectives. Hence, different approaches were used to obtain the sequence data. For the little eagle and booted eagle, DNA from blood extracts was prepared for high throughput sequencing by the sequencing service of New Zealand Genomics Limited (NZGL) using a TruSeq library preparation kit and following the manufacturer's instructions. Sequencing libraries were prepared directly from the DNA extracts and libraries were not enriched prior to sequencing. For the spotted harrier, we amplified the complete mitogenome in two long range amplifications using KAPA Long range PCR enzyme with an annealing temperature of 50C and following the manufacturer's recommendations for a thermal profile. (see supplementary table S2 for primers used). PCR products were purified using Mag-Bind magnetic beads in 1:1 ratio following the manufacturer's instructions and both long range products were pooled in equimolar ratios after Qubit quantification. The pool of long-range amplicons was then sheared into 500 bp fragments on a Bioruptor DNA sonicator. A sequencing library was produced from the fragmented pool of amplicons following Clarke et al. (2014).

An Illumina sequencing library was prepared from the DNA of Eyles' harrier using a single-stranded library preparation protocol for degraded DNA as described by Gansauge and Meyer (2013). Twenty µL of DNA extract were used to start the preparation and completed libraries were eluted in 25 µL of 1× TET buffer (TE + 0.05% Tween-20) after amplification of the adapter-ligated library and a final Qiagen Minelute purification step. The sequencing library was not enriched prior to sequencing.

An Illumina sequencing library were prepared from Haast's eagle DNA using the NEBNext® DNA Library Prep Master Mix Set and following manufacturer's instructions, with the replacement of 454 adapters with Illumina adapters. Instead of using magnetic beads, clean-up was performed using Qiagen silica columns. Thirty µl of DNA extract were used to start the preparation and completed libraries were eluted in 62 µL of 1x TE buffer after amplification of the adapter ligated library and a final Qiagen Minelute purification step. The sequencing library was enriched for Haast's eagle mitochondrial DNA using MYcroarray myBait RNA probes following the manufacturer's instructions. The RNA probes were designed from the little eagle mitogenome sequence obtained during this study. Sequencing libraries were sequenced either by themselves or with other samples on Illumina MiSeq

or HiSeq platforms.

2.3. Mapping and consensus calling

2.3.1. Little eagle and booted eagle

In order to reconstruct the mitogenomes of the little and the booted eagle, we compared three assembly approaches for each species: one reference based assembly and two *de novo* assemblies. For the reference-based assembly of little eagle and booted eagle mitogenomes, we used bowtie2 (option –local) (Langmead and Salzberg, 2012) to map genomic DNA reads against the complete mitogenome of the mountain hawk-eagle (NC_007598), which was the most closely related species to Little Eagle and Booted Eagle with a published mitogenome at the time. The resulting SAM file for each species was then processed and the respective consensus called using the mpileup function in samtools (Li et al., 2009). For the two *de novo* assemblies, we used the assemblers Allpaths-LG (partial assembly) (Gnerre et al., 2011) and PRICE (Ruby et al., 2013) respectively.

The reconstructed reference-based consensus sequences matched the respective partial consensuses generated using Allpaths-LG, but showed a few differences from the PRICE assemblies. Both the reference-based and the Allpaths-LG consensuses showed higher support by the mapped reads (number of reads and alignment breakpoints; in both species) than the PRICE assemblies. We used the reference-based consensus sequences for all downstream analyses, because they were more continuous than the Allpaths-LG assemblies.

2.3.2. Spotted harrier

After removing the sequencing adapters, we used Geneious 10.0.9 (Kearse et al., 2012) to map the FASTQ data from Illumina sequencing of sheared long-range PCR amplicons from the spotted harrier against the besra mitogenome (GenBank accession number NC_026082.1). A consensus was called for all positions with at least 5× coverage using a majority rule consensus, with ambiguous and low-coverage positions called as 'undetermined' (N).

2.3.3. Haast's eagle and Eyles' harrier

The FASTQ data from Illumina sequencing of Haast's eagle and Eyles' harrier were processed with AdapterRemoval (Lindgreen, 2012). Mitogenomes were assembled using the BWA aln algorithm (Li and Durbin, 2009) and slightly modified default settings with deactivated seeding (−l 16,500), allowing more substitutions (−n 0.01), and allowing up to two gaps (−o 2). The BWA samse command was used to generate alignments.

Reads from Haast's eagle were mapped against a hybrid mitogenome from little eagle and Haast's eagle that was produced by mapping all sequencing reads from five Haast's eagle individuals (including the one presented in this study) against the little eagle mitogenome assembled as described above. To assemble the hybrid reference genome, a consensus of Haast's eagle reads was called and complemented with little eagle sequence data where no Haast's eagle reads were available. Haast's eagle reads were also mapped against the little eagle and booted eagle mitogenomes, but this yielded slightly less coverage than mapping against the hybrid mitogenome (123× for hybrid, 107× for little eagle and 105× for booted eagle as reference). Eyles' harrier reads were mapped against the spotted harrier mitogenome which had been assembled as described above.

Reads mapping to the respective mitochondrial reference genome were extracted and processed in SAMtools, including converting the alignments from SAM format to BAM format, as well as coordinate sorting, indexing, and removing duplicates from the alignments. Reads with mapping qualities below 30 were filtered out. A consensus was called using Geneious for all positions with at least 5× coverage using the majority rule consensus, with ambiguous and low-coverage positions called as 'undetermined' (N). For the Eyles' harrier, sequencing gaps in the Sanger sequenced *ND1* and surrounding regions were filled with Sanger sequencing data if they were unambiguous. The average coverage was estimated using the samtools depth command. Finally, we used MapDamage 2.0 (Jónsson et al., 2013) to examine patterns of deamination at sequencing read beginnings and other nucleotide misincorporations, which are typical of ancient DNA due to degradation (supplementary Fig. S1).

2.4. Phylogenetic analyses of extant harriers and Eyles' harrier

In order to infer the phylogenetic position of Eyles's harrier, we aligned sequences of tRNA-Leu, *ND1*, tRNA-Ile, and tRNA-Gln to the corresponding sequences from all extant harriers as presented by Oatley et al. (2015). Phylogenetic relationships were inferred using maximum likelihood in the software RAxML 8.2.7 (Stamatakis, 2014) as well as a Bayesian approach in MrBayes 3.2.6 (Ronquist et al., 2012). The TrN + I model of nucleotide substitution was selected using the Bayesian information criterion in jModeltest 2 (Darriba et al., 2012). In our analyses, we used the closest pre-defined substitution models available, which are GTR + I + G in RAxML and GTR + I in MrBayes. For the maximum-likelihood analyses we used a randomized stepwise-addition parsimony starting tree. Branch support was evaluated with 1000 bootstrap pseudoreplicates. Bayesian phylogenetic analyses were conducted with four Markov chains, three of them heated. Chain lengths were 1.1 million steps with every 200th step being sampled, and with the first 100,000 steps discarded as burn-in. Analyses were run twice and convergence of the Markov Chain as well as the effective sample sizes for all parameters were checked in Geneious. Effective sample sizes for al parameters greatly exceeded 200 in all cases, confirming a sufficient chain length. Phylogenetic trees were visualized using FigTree 1.4.3 (Rambaut, 2009).

2.5. Phylogenetic analysis and molecular dating of mitogenomes

We obtained all available complete mitogenome sequences of Accipitriformes from GenBank and randomly selected one sequence from each species. Combined with the new mitogenome sequences, this yielded a data set comprising sequences from 22 accipitrid species and three other accipitriforms (Supplementary Table S3): Osprey (*Pandion haliaetus*, Pandionidae), Secretarybird (*Sagittarius serpentarius*, Sagittaridae), and Turkey Vulture (*Cathartes aura*, Cathartidae). To avoid ambiguities from poorly aligning intergene regions, phylogenetic analyses were limited to genes. The sequences of 37 genes were extracted from each mitogenome, comprising 13 protein-coding genes, two rRNA genes, and 22 tRNA genes. Sequences were aligned for each gene using MUSCLE (Edgar, 2004).

We compared the fit of five data-partitioning schemes, two clock models (strict clock and uncorrelated lognormal relaxed clock; Drummond et al., 2006), and two tree priors (Yule process and birth-death process). Models were compared using marginal likelihoods calculated via stepping-stone analysis with 25 path samples (Xie et al., 2011). A partitioning scheme with five partitions, an uncorrelated lognormal relaxed clock, and a Yule tree prior yielded the highest marginal likelihood (Table S5).

Consequently the alignments were concatenated to form five data partitions, comprising the three codon positions of the protein-coding genes, the rRNA genes, and the tRNA genes. For each of the five partitions, we used the Bayesian information criterion in Modelgenerator (Keane et al., 2006) to select the best-fitting model of nucleotide substitution. Using 100 predictive simulations in PhyloMAd (Duchêne et al., 2018), we confirmed the adequacy of using a homogeneous substitution model for each partition. The chi-squared test statistic indicated a low risk of phylogenetic bias due to compositional heterogeneity among the sequences (Duchêne et al., 2017).

To infer the evolutionary relationships among the 25 mitogenomes, we performed a maximum-likelihood phylogenetic analysis using RAxML (Stamatakis, 2014). The data set was partitioned as described

above and a GTR + G substitution model was applied to each partition. To infer node support values, a rapid bootstrapping analysis with 1000 replicates was performed. These replicates were used to provide starting points for searches for the best-scoring tree. The tree was rooted by treating the Turkey Vulture (*Cathartes aura*) as the sister lineage to all other taxa in the data set, based on a previous estimate of the bird phylogeny (Prum et al., 2015).

We inferred the evolutionary relationships and timescale using a Bayesian phylogenetic analysis in BEAST 1.8.4 (Drummond et al., 2012). Our estimate of the timescale was calibrated using a previous genome-scale estimate for the divergence time between *Cathartes aura* and the remaining accipitriform species (Jarvis et al., 2014). This date estimate was used to specify a normal prior on the age of the root, with a mean of 60.34 Ma and standard deviation of 1.61 Ma. A continuous-time Markov chain reference prior was used for the mean substitution rate (Ferreira and Suchard, 2008), with a separate relative-rate parameter assigned to each data subset.

The posterior distribution was estimated by Markov chain Monte Carlo (MCMC) sampling, with samples drawn every 5000 steps from a total of 50 million MCMC steps. To check for convergence to the stationary distribution, we ran each MCMC analysis in duplicate. To check for sufficient sampling, we used Tracer 1.7 (Rambaut et al., 2018) to confirm that the effective sample size for each model parameter was greater than 200.

3. Results

3.1. Sequence data

Complete high-quality mitogenome sequences were obtained from one sample of Haast's eagle (123× unique coverage), little eagle (170×), booted eagle (238×), and Eyles' harrier (23×) and spotted harrier (779×). Sequence data from Eyles' harrier and Haast's eagle were checked for deamination damage at the 5′ and 3′ ends of molecules, which is a damage pattern characteristic of ancient DNA. As expected, the sequence data showed this characteristic damage pattern (supplementary Fig. S1).

We performed phylogenetic analyses of the mitochondrial fragment covering 1027 bp of tRNA-Leu, *ND1*, tRNA-Ile, and tRNA-Gln. For this section of the mitochondrial genome, Eyles' harrier is most similar to the Australasian spotted harrier (97.2% identical; supplementary table S6). Eyles' harrier was grouped with spotted harrier in our phylogenetic analyses using maximum likelihood (97% bootstrap support) and Bayesian inference (posterior probability 1.00) (Fig. 1).

Our analyses of mitogenomic data confirmed the relationships that had been expected from analyses of shorter mitochondrial fragments (this study and (Bunce et al., 2005)) (Fig. 2). Haast's eagle grouped with the Australasian little eagle, whereas Eyles' harrier grouped with the Australasian spotted harrier. Node posterior probabilities and bootstrap support were high across the phylogeny (Fig. 2). The two divergences between the small Australian species and their giant sister taxa from New Zealand were estimated to have occurred at similar times. Eyles' harrier diverged from the spotted harrier 2.37 Ma (95% credibility interval 1.40–3.54 Ma), whereas Haast's eagle diverged from the little eagle 2.22 Ma (95% credibility interval 1.41–3.25 Ma). These fossil calibrated estimates for Haast's eagle are nearly twice as old as those provided by Bunce et al. (2005) based on a small fragment of the mitochondrial genome and a general avian substitution rate (0.7–1.8 Ma), highlighting the variation in substitution rates between species (Nabholz et al., 2016). Nevertheless, both estimates confirm a Pleistocene divergence between little eagle and Haast's eagle.

4. Discussion

The phylogenetic relationships of New Zealand's second largest extinct avian predator, the Eyles' harrier have been unclear. Worthy & Holdaway (2002) hypothesised that of the two harrier species that breed closest to New Zealand, the mid-sized spotted harrier (up to 750 g) and the larger swamp harrier (*Circus approximans*, up to 1.1 kg), the latter was most likely to share a close relationship with Eyles' harrier. This was not only suggested by the size but also by the fact that the swamp harrier is the only *Circus* sp. to have reached other Pacific islands and has successfully self-dispersed to New Zealand – presumably using the prevailing west-east air flow (Sanmartín et al., 2007). However, our phylogenetic analyses show a close relationship between New Zealand's extinct Eyles' harrier and the Australasian spotted harrier (for the purpose of this discussion 'Australasia' is excluding New Zealand). The early Pleistocene timing of the divergence between these species is strikingly similar to that of the split between the New Zealand Haast's eagle and its Australasian relative, the little eagle. Here we discuss both the evolutionary and the biogeographic implications of our findings.

4.1. The evolution of island gigantism in New Zealand raptors

Haast's eagle is estimated to have been a staggering 15 times heavier than its close Australasian relative (Bunce et al., 2005), while Eyles' harrier was a more moderate 4.5 times larger than its closest relative from across the Tasman (Worthy and Holdaway, 2002). Nevertheless, given the short evolutionary time scale of likely less than 2.5 million years separating the species, the size differences are significant. The only other Australia-New Zealand bird species pair with similar divergence times and size differences are the Australasian pukeko (up to 1 kg), and the New Zealand takahe, the largest rail in the world at up to 3.5 kg (Garcia-Ramirez and Trewick, 2015).

To discuss the rapid evolution of island gigantism in New Zealand birds of prey, two key questions need to be addressed: What was the size of the common ancestor of New Zealand island giant and their Australian relative compared to its descendants and where did this common ancestor live? Haast's eagle is phylogenetically nested within a group of small eagles (Bunce et al., 2005), and we may therefore assume that its ancestor was a relatively small eagle as well. Similarly, Eyles' harrier is unique among harriers in that it is more than three times the size of the currently largest harrier, the swamp harrier, again suggesting that its giant size evolved in New Zealand from a smaller Australian ancestor. However, cases of bird taxa shrinking in size in Australia since the Pleistocene have for example been reported from coucals (Shute et al., 2016). We therefore cannot completely reject the possibility that some of the size differences between little eagle, spotted harrier and their respective island giant relative could be owed to a reduction in size in the Australasian species.

Our genetic data does not provide any information about the range and origin of the common ancestors of Australasian and New Zealand raptors. It does not help to distinguish whether the species originated in New Zealand and dispersed to Australia, or dispersed to New Zealand. However, empirical data provides evidence of a very clear trend. For example, within the last 700 years alone, at least 16 Australian bird species dispersed to and established in New Zealand (Waters and Grosser, 2016). In contrast, no case of New Zealand endemic or native bird species (previously absent from Australia) having dispersed to and established in Australia is known from the same time period. It is likely that the westerly winds over the Tasman Sea, which have already been predominant in the early Pleistocene when the ancestors of Eyles' harrier and Haast's eagle reached New Zealand, reduce the number of New Zealand vagrants reaching Australia, thereby also reducing the likelihood of successful establishment (Sanmartín et al., 2007). Considering all available evidence, the most likely biogeographic and evolutionary history of New Zealand's giant raptors is therefore that they are descendant of a smaller Australasian species that dispersed to New Zealand. Once in New Zealand, the absence of mammalian predators and presence of large avian herbivores would have facilitated a rapid size increase to adapt to the niche of apex predator (Bunce et al., 2005).

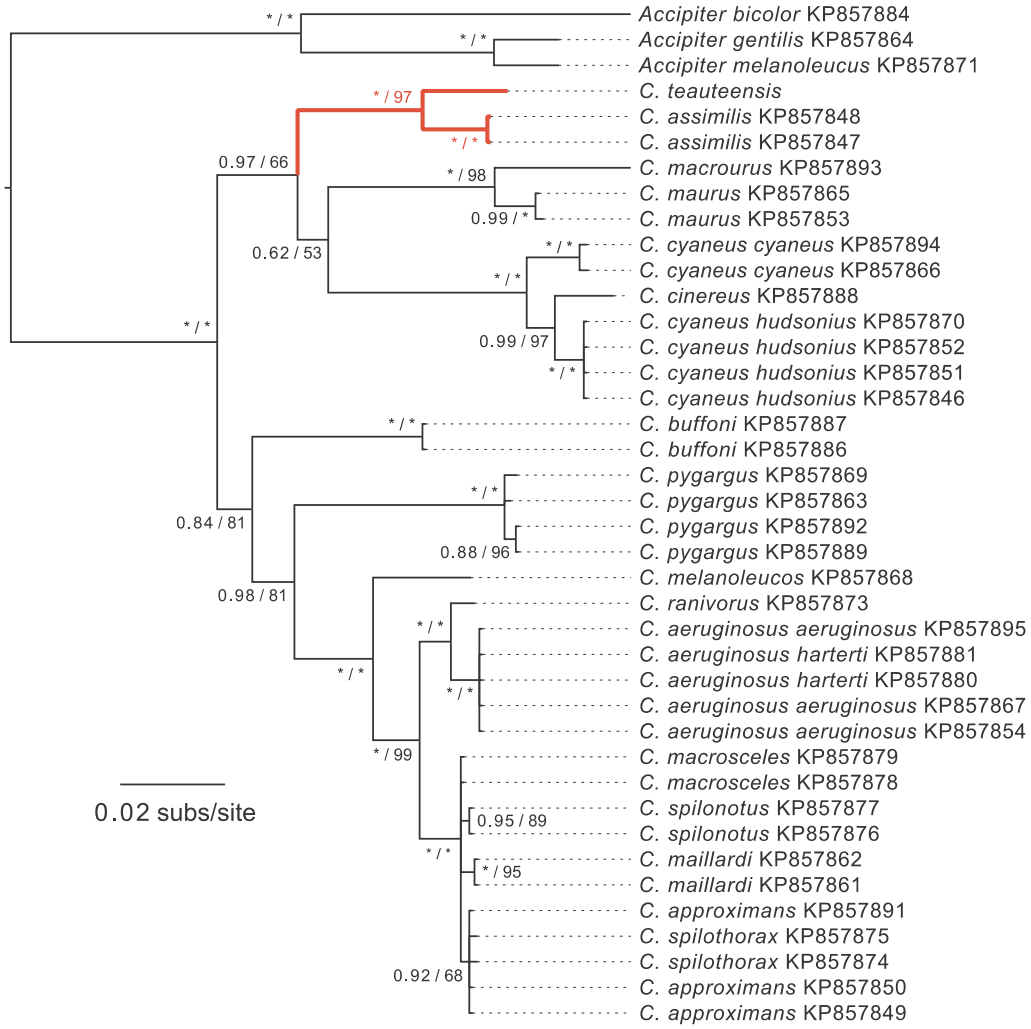

Fig. 1. Bayesian phylogeny of the genus *Circus* inferred from mitochondrial tRNA-Leu, *ND1*, tRNA-Ile, and tRNA-Gln regions (1027 bp). The placement of the root was inferred by treating three species of *Accipiter* as the outgroup. Nodes are labelled with posterior probabilities/ bootstrap support. * represents a posterior probability of 1 and a bootstrap support of 100 respectively. The scale bar represents 0.02 substitutions per site.

4.2. The biogeographic history of New Zealand's extinct giant raptors

Two key factors determine the ability of species to establish populations on an isolated island. First, a sufficient number of individuals need to reach the island. Second, the population then needs to survive and reproduce in the new habitat. Thus, mobility and competitiveness of a species in the new environment determine whether or not a species will establish successfully (Waters, 2011). For birds, the Tasman Sea between Australia and New Zealand is a barrier to dispersal, but one that many volant species have overcome. Species that have successfully self-dispersed across the Tasman Sea and established in New Zealand in the past 700 years include for example pied stilt (*Himantopus leucocephalus*), purple swamp hen/pukeko (*Porphyrio melanotus*), welcome swallow (Hirundo neoxena), white eye (*Zosterops lateralis*) and the swamp harrier (*Circus approximans*) (16 species in total; Waters and Grosser, 2016).

Successful establishment is thereby a much greater challenge than just dispersal, because of the differing habitats of Australia and New Zealand in the past. Both Australian relatives of New Zealand's giant raptors are species of open woodlands and grasslands, while New Zealand was densely forested for most of the last 20 million years (Fleming, 1979; Mildenhall, 1980). Open woodlands and grasslands are likely to have increased significantly only at the onset of Pleistocene glaciations in New Zealand about 2.5 Ma (Fleming, 1979; Heenan and McGlone, 2013; Mildenhall, 1980). This date is consistent with the times that we estimated for the divergences between Eyles' harrier and spotted harrier (2.4 Ma) and between Haast's eagle and little eagle (2.2 Ma). This finding suggests that the deforestation associated with the onset of glacial climates may have provided a window for open land adapted migrants from Australia to establish in New Zealand.

Pleistocene divergences between New Zealand and Australian taxa have also been reported for black stilt (*Himantopus novaezelandiae*) and pied stilt (*Himantopus leucocephalus*) (Wallis, 1999), Takahe (*Porphyrio hochstetteri*) and Pukeko (*Porphyrio porphyrio melanotus*) (Garcia-R. and Trewick, 2015), and New Zealand raven (*Corvus antipodum*) and Australian raven (*Corvus coronoides*) clade (Scofield et al., 2017). It is possible that the above species pairs as well as Eyles' harrier and Haast's eagle are examples of a much broader pattern of Pleistocene dispersal from Australia to New Zealand, facilitated by the environmental changes associated with the onset of the ice ages. A more extensive study of divergence times of Australia-New Zealand sister taxa would be required to test this hypothesis.

5. Conclusions

Our study provides evidence of a rapid evolution of island gigantism of birds of prey in New Zealand. It also puts the evolution of these island giants into context of the evolution of other, contemporaneous

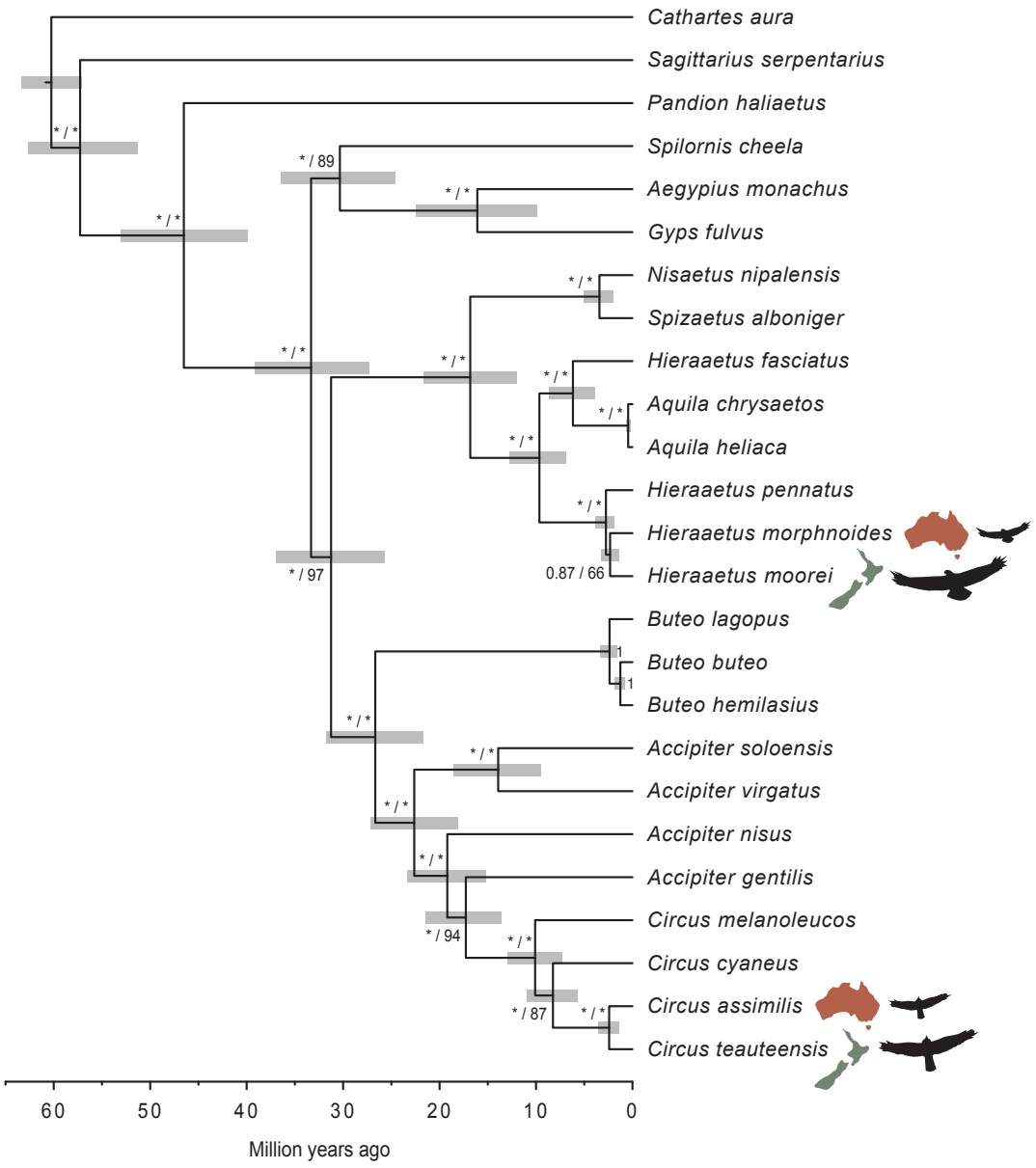

Fig. 2. Bayesian phylogenetic tree showing divergence times of the New Zealand island giants from their closest, small-sized Australian relatives. Nodes are labelled with posterior probabilities/ bootstrap support. * represents a posterior probability of 1 and a bootstrap support of 100 respectively. Horizontal grey bars indicate 95% credibility intervals of node-age estimates.

migrants to New Zealand. Neither stilts nor ravens - for example - went through comparably dramatic phenotypic changes in adaptation to New Zealand environments. Only functional genomic studies will be able to evaluate whether such dramatic phenotypic changes have to be accompanied by dramatic genomic changes. Further work will also be valuable for testing our proposed explanations for the divergence times between New Zealand island giants and their smaller-sized Australian relatives.

Acknowledgements

We thank the International Centre for Birds of Prey in Newent, UK, the Perth Raptor Care (Marra Apgar) and the Australian National Wildlife Collection (CSIRO, Canberra) for providing samples for this study. MK is supported by a Rutherford Discovery Fellowship from the Royal Society of New Zealand (14-UOO-007). JET was supported by the Natural Environment Research Council (NERC) grant NE/L501694/1. MTPG is supported by ERC Consolidator grant 681396-EXTINCTION GENOMICS.

Competing interests

We have no competing interests.

Authors' contributions

All authors contributed to writing the manuscript. MK and RPS designed the study. MK, JET, and JH conducted laboratory work and analysed data, SP, SYWH, ND, and SC-C analysed data, OK and RB conducted laboratory work, MB contributed materials, MTPG coordinated laboratory work and analyses.

Appendix A. Supplementary material

Supplementary data to this article can be found online at https://doi.org/10.1016/j.ympev.2019.01.026.

References

Bunce, M., Szulkin, M., Lerner, H.R.L., Barnes, I., Shapiro, B., Cooper, A., Holdaway, R.N., 2005. Ancient DNA provides new insights into the evolutionary history of New Zealand's extinct giant eagle. PLoS Biol. 3, e9. https://doi.org/10.1371/journal.pbio.0030009.

Clarke, A.C., Prost, S., Stanton, J.A.L., White, W.T.J., Kaplan, M.E., Matisoo-Smith, E.A., Adhikarla, S., Adler, C.J., Balanovska, E., Balanovsky, O., Bertranpetit, J., Comas, D., Cooper, A., Der Sarkissian, C.S.I., Dulik, M.C., Gaieski, J.B., GaneshPrasad, A.K., Haak, W., Haber, M., Jin, L., Li, S., Martínez-Cruz, B., Merchant, N.C., Mitchell, R.J., Owings, A.C., Parida, L., Pitchappan, R., Platt, D.E., Quintana-Murci, L., Renfrew, C., Lacerda, D.R., Royyuru, A.K., Santos, F.R., Schurr, T.G., Soodyall, H., Hernanz, S., Swamikrishnan, P., Tyler-Smith, C., Santhakumari, A.V., Vieira, P.P., Vilar, M.G., Zalloua, P.A., Ziegle, J.S., Wells, R.S., 2014. From cheek swabs to consensus sequences: An A to Z protocol for high-throughput DNA sequencing of complete human mitochondrial genomes. BMC Genomics 15, 1–12. https://doi.org/10.1186/1471-2164-15-68.

Dabney, J., Knapp, M., Glocke, I., Gansauge, M.-T., Weihmann, A., Nickel, B., Valdiosera, C., García, N., Pääbo, S., Arsuaga, J.-L., Meyer, M., 2013. Complete mitochondrial genome sequence of a Middle Pleistocene cave bear reconstructed from ultrashort DNA fragments. Proc. Natl. Acad. Sci. U.S.A. 110, 15758–15763. https://doi.org/10.1073/pnas.1314445110.

Darriba, D., Taboada, G.L., Doallo, R., Posada, D., 2012. jModelTest 2: more models, new heuristics and parallel computing. Nat. Methods 9, 772. https://doi.org/10.1038/nmeth.2109.

Drummond, A.J., Ho, S.Y.W., Phillips, M.J., Rambaut, A., 2006. Relaxed phylogenetics and dating with confidence. PLoS Biol. 4, 699–710. https://doi.org/10.1371/journal.pbio.0040088.

Drummond, A.J., Suchard, M.A., Xie, D., Rambaut, A., 2012. Bayesian phylogenetics with BEAUti and the BEAST 1.7. Mol. Biol. Evol. 29, 1969–1973. https://doi.org/10.1093/molbev/mss075.

Duchêne, D.A., Duchêne, S., Ho, S.Y.W., 2017. New statistical criteria detect phylogenetic bias caused by compositional heterogeneity. Mol. Biol. Evol. 34, 1529–1534. https://doi.org/10.1093/molbev/msx092.

Duchêne, D.A., Ho, S.Y.W., Duchêne, S., 2018. PhyloMAd: Efficient assessment of phylogenomic model adequacy. Bioinformaticstics in press.

Edgar, R.C., 2004. MUSCLE: Multiple sequence alignment with high accuracy and high throughput. Nucleic Acids Res. 32, 1792–1797. https://doi.org/10.1093/nar/gkh340.

Ferreira, M.A.R., Suchard, M.A., 2008. Bayesian analysis of elapsed times in continuous-time Markov chains. Can. J. Stat. 36, 355–368. https://doi.org/10.1002/cjs.5550360302.

Fleming, C.A., 1979. The Geological History of New Zealand and its Life. Auckland University Press, Auckland.

Gansauge, M.-T., Meyer, M., 2013. Single-stranded DNA library preparation for the sequencing of ancient or damaged DNA. Nat. Protoc. 8, 737–748. https://doi.org/10.1038/nprot.2013.038.

Garcia-Ramirez, J.C., Trewick, S.A., 2015. Dispersal and speciation in purple swamphens (Rallidae: *Porphyrio*). Auk 132, 140–155. https://doi.org/10.1642/AUK-14-114.1.

Gnerre, S., MacCallum, I., Przybylski, D., Ribeiro, F.J., Burton, J.N., Walker, B.J., Sharpe, T., Hall, G., Shea, T.P., Sykes, S., Berlin, A.M., Aird, D., Costello, M., Daza, R., Williams, L., Nicol, R., Gnirke, A., Nusbaum, C., Lander, E.S., Jaffe, D.B., 2011. High-quality draft assemblies of mammalian genomes from massively parallel sequence data. Proc. Natl. Acad. Sci. 108, 1513–1518. https://doi.org/10.1073/pnas.1017351108.

Heenan, P.B., McGlone, M.S., 2013. Evolution of New Zealand alpine and open-habitat plant species during the late Cenozoic. N. Z. J. Ecol. 37, 105–113.

Jarvis, E.D., Mirarab, S., Aberer, A.J., Li, B., Houde, P., Li, C., Ho, S.Y.W., Faircloth, B.C., Nabholz, B., Howard, J.T., Suh, A., Weber, C.C., da Fonseca, R.R., Li, J., Zhang, F., Li, H., Zhou, L., Narula, N., Liu, L., Ganapathy, G., Boussau, B., Bayzid, M.S., Zavidovych, V., Subramanian, S., Gabaldón, T., Capella-Gutiérrez, S., Huerta-Cepas, J., Rekepalli, B., Munch, K., Schierup, M., Lindow, B., Warren, W.C., Ray, D., Green, R.E., Bruford, M.W., Zhan, X., Dixon, A., Li, S., Li, N., Huang, Y., Derryberry, E.P., Bertelsen, M.F., Sheldon, F.H., Brumfield, R.T., Mello, C.V., Lovell, P.V., Wirthlin, M., Schneider, M.P.C., Prosdocimi, F., Samaniego, J.A., Vargas Velazquez, A.M., Alfaro-Núñez, A., Campos, P.F., Petersen, B., Sicheritz-Ponten, T., Pas, A., Bailey, T., Scofield, P., Bunce, M., Lambert, D.M., Zhou, Q., Perelman, P., Driskell, A.C., Shapiro, B., Xiong, Z., Zeng, Y., Liu, S., Li, Z., Liu, B., Wu, K., Xiao, J., Yinqi, X., Zheng, Q., Zhang, Y., Yang, H., Wang, J., Smeds, L., Rheindt, F.E., Braun, M., Fjeldsa, J., Orlando, L., Barker, F.K., Jønsson, K.A., Johnson, W., Koepfli, K.-P., O'Brien, S., Haussler, D., Ryder, O.A., Rahbek, C., Willerslev, E., Graves, G.R., Glenn, T.C., McCormack, J., Burt, D., Ellegren, H., Alström, P., Edwards, S.V., Stamatakis, A., Mindell, D.P., Cracraft, J., Braun, E.L., Warnow, T., Jun, W., Gilbert, M.T.P., Zhang, G., 2014. Whole-genome analyses resolve early branches in the tree of life of modern birds. Science 346, 1320–1331. https://doi.org/10.1126/science.1253451.

Jónsson, H., Ginolhac, A., Schubert, M., Johnson, P.L.F., Orlando, L., 2013. mapDamage2.0: fast approximate Bayesian estimates of ancient DNA damage parameters. Bioinformatics 29, 1682–1684. https://doi.org/10.1093/bioinformatics/btt193.

Keane, T.M., Creevey, C.J., Pentony, M.M., Naughton, T.J., Mclnerney, J.O., 2006. Assessment of methods for amino acid matrix selection and their use on empirical data shows that ad hoc assumptions for choice of matrix are not justified. BMC Evol. Biol. 6, 29. https://doi.org/10.1186/1471-2148-6-29.

Kearse, M., Moir, R., Wilson, A., Stones-Havas, S., Cheung, M., Sturrock, S., Buxton, S., Cooper, A., Markowitz, S., Duran, C., Thierer, T., Ashton, B., Meintjes, P., Drummond, A., 2012. Geneious Basic: an integrated and extendable desktop software platform for the organization and analysis of sequence data. Bioinformatics 28, 1647–1649. https://doi.org/10.1093/bioinformatics/bts199.

Knapp, M., Clarke, A.C., Horsburgh, K.A., Matisoo-Smith, E.A., 2012. Setting the stage – Building and working in an ancient DNA laboratory. Ann. Anat. - Anat. Anzeiger 194, 3–6. https://doi.org/10.1016/j.aanat.2011.03.008.

Langmead, B., Salzberg, S.L., 2012. Fast gapped-read alignment with Bowtie 2. Nat. Methods 9, 357–359. https://doi.org/10.1038/nmeth.1923.

Leonard, J.A., Wayne, R.K., Cooper, A., 2000. Population genetics of Ice Age brown bears. Proc. Natl. Acad. Sci. 97, 1651–1654. https://doi.org/10.1073/pnas.040453097.

Li, H., Durbin, R., 2009. Fast and accurate short read alignment with Burrows-Wheeler transform. Bioinformatics 25, 1754–1760. https://doi.org/10.1093/bioinformatics/btp324.

Li, H., Handsaker, B., Wysoker, A., Fennell, T., Ruan, J., Homer, N., Marth, G., Abecasis, G., Durbin, R., 2009. The Sequence Alignment/Map format and SAMtools. Bioinformatics 25, 2078–2079. https://doi.org/10.1093/bioinformatics/btp352.

Lindgreen, S., 2012. Adapterremoval: easy cleaning of next generation sequencing reads. BMC Res. Notes 5, 337. https://doi.org/10.1186/1756-0500-5-337.

Mildenhall, D.C., 1980. New Zealand Late Cretaceous and Cenozoic plant biogeography: A contribution. Palaeogeogr. Palaeoclimatol. Palaeoecol. 31, 197–233.

Nabholz, B., Lanfear, R., Fuchs, J., 2016. Body mass-corrected molecular rate for bird mitochondrial DNA. Mol. Ecol. 25, 4438–4449. https://doi.org/10.1111/mec.13780.

Oatley, G., Simmons, R.E., Fuchs, J., 2015. A molecular phylogeny of the harriers (Circus, Accipitridae) indicate the role of long distance dispersal and migration in diversification. Mol. Phylogenet. Evol. 85, 150–160. https://doi.org/10.1016/j.ympev.2015.01.013.

Prum, R., Berv, J., Dornburg, A., Field, D., Townsend, J., Moriarty Lemmon, E., Lemmon, A., 2015. A comprehensive phylogeny of birds (Aves) using targeted next-generation DNA sequencing. Nature 526, 569–573.

Rambaut, A., 2009. FigTree: Tree figure drawing tool, v1.4.3.

Rambaut, A., Drummond, A., Xie, D., Baele, G., Suchard, M., 2018. Posterior summarisation in Bayesian phylogenetics using Tracer 1.7. Syst. Biol (in press).

Ronquist, F., Teslenko, M., Van Der Mark, P., Ayres, D.L., Darling, A., Höhna, S., Larget, B., Liu, L., Suchard, M.A., Huelsenbeck, J.P., 2012. MrBayes 3.2: Efficient bayesian phylogenetic inference and model choice across a large model space. Syst. Biol. 61, 539–542. https://doi.org/10.1093/sysbio/sys029.

Ruby, J.G., Bellare, P., DeRisi, J.L., 2013. PRICE: Software for the Targeted Assembly of Components of (Meta) Genomic Sequence Data. G3: Genes|Genomes|Genetics 3, 865–880. https://doi.org/10.1534/g3.113.005967.

Sanmartín, I., Wanntorp, L., Winkworth, R.C., 2007. West wind drift revisited: Testing for directional dispersal in the southern hemisphere using event-based tree fitting. J. Biogeogr. 34, 398–416. https://doi.org/10.1111/j.1365-2699.2006.01655.x.

Scofield, R.P., Mitchell, K.J., Wood, J.R., De Pietri, V.L., Jarvie, S., Llamas, B., Cooper, A., 2017. The origin and phylogenetic relationships of the New Zealand ravens. Mol. Phylogenet. Evol. 106, 136–143. https://doi.org/10.1016/j.ympev.2016.09.022.

Shute, E., Prideaux, G.J., Worthy, T.H., 2016. Three terrestrial Pleistocene coucals (*Centropus*: Cuculidae) from southern Australia: biogeographical and ecological significance. Zool. J. Linn. Soc. 177, 964–1002. https://doi.org/10.1111/zoj.12387.

Stamatakis, A., 2014. RAxML version 8: a tool for phylogenetic analysis and post-analysis of large phylogenies. Bioinformatics 30, 1312–1313. https://doi.org/10.1093/bioinformatics/btu033.

Wallis, G., 1999. Genetic status of New Zealand black stilt (*Himantopus novaezelandiae*) and impact of hybridisation. Conserv. Advis. Sci. Notes 239.

Waters, J.M., 2011. Competitive exclusion: Phylogeography's "elephant in the room"? Mol. Ecol. 20, 4388–4394. https://doi.org/10.1111/j.1365-294X.2011.05286.x.

Waters, J.M., Grosser, S., 2016. Managing shifting species: Ancient DNA reveals conservation conundrums in a dynamic world. BioEssays 38, 1177–1184. https://doi.org/10.1002/bies.201600044.

Wood, J.R., Scofield, R.P., Hamel, J., Lalas, C., Wilmshurst, J.M., 2017. Bone stable isotopes indicate a high trophic position for new zealand's extinct south island adzebill (*Aptornis defossor*) (Gruiformes: Aptornithidae). N. Z. J. Ecol. 41, 240–244. https://doi.org/10.20417/nzjecol.41.24.

Worthy, T.H., 1997. Quaternary fossil fauna of South Canterbury, South Island, New Zealand. J. R. Soc. New Zeal. 27, 67–162. https://doi.org/10.1080/03014223.1997.9517528.

Worthy, T.H., Holdaway, R.N., 2002. The lost world of the moa : prehistoric life of New Zealand. Indiana University Press.

Xie, W., Lewis, P.O., Fan, Y., Kuo, L., Chen, M.-H., 2011. Improving Marginal Likelihood Estimation for Bayesian Phylogenetic Model Selection. Syst. Biol. 60, 150–160. https://doi.org/10.1093/sysbio/syq085.